Hindawi
Journal of Chemistry
Volume 2022, Article ID 7010428, 7 pages
https://doi.org/10.1155/2022/7010428

Research Article

Investigation of Cinnamaldehyde Derivatives as Potential Organic UV Filters

Monica B. Pan, Chloe S. Hughes, Hailey N. Lynch, Marcia M. Schilling, and Anuradha Liyana Pathiranage

Austin Peay State University, Clarksville, TN 37044, USA

Correspondence should be addressed to Anuradha Liyana Pathiranage; pathiranagea@apsu.edu

Received 5 September 2021; Revised 8 February 2022; Accepted 17 February 2022; Published 14 March 2022

Academic Editor: Khaled Mostafa

Long-term exposure to ultraviolet (UV) rays has been attributed to irreversible health defects at the cellular level. Most importantly, damage to DNA by UVA and UVB rays can result in uncontrolled cellular growth, leading to skin cancer. As a result, topical treatments have been developed over time to protect the skin from UVA and UVB rays. The active ingredients in sunscreens or sun creams are sometimes unsaturated, aromatic organic compounds capable of absorbing harmful UV photons at a great range of wavelengths. Absorption capabilities of these species depend on their degree of conjugation and their molar absorptivity. With this knowledge, two cinnamaldehyde derivatives were synthesized into five potential organic UV filters by the aldol condensation reaction. The products were identified using nuclear magnetic resonance (NMR) and attenuated total reflection Fourier-transform infrared (ATR-FTIR) spectroscopies, and ultraviolet-visible (UV-vis) spectroscopy was used to determine the UV absorption range and intensity of absorption for each compound. Since the compounds would hypothetically be utilized in topical ointments to aide in skin protection, these compounds were assessed in the presence of *Pseudomonas aeruginosa*, a representative bacterium of the skin's natural flora. A time-course assay was conducted to detect growth effects of *P. aeruginosa* in the presence of the organic compounds. According to the spectroscopic and bacterial analyses of these UV-blocking compounds, three compounds were determined to be potential UV filters that cover UVA region while demonstrating no apparent harm to the natural skin bacteria *P. aeruginosa,* while the other two likely diminished bacterial growth by simple niche inhibition.

1. Introduction

Sunlight exposure is valued for its benefits to human health, especially its role in the synthesis of vitamin D from cholesterol. Unfortunately, prolonged and unprotected exposure to UV rays has been associated with irreversible health defects [1]. The region of UV light emitted by the sun is categorized into three types, which span the following wavelengths: UVA (320–400 nm), UVB (290–320 nm), and UVC (200–290 nm) [2]. Essentially, all UVC rays and a significant portion of UVB rays are absorbed by Earth's atmosphere and do not penetrate its surface. As a result, UVC ranges of UV light are not typically considered when investigating potential UV filters. Since both UVB and UVA radiation can reach the Earth's surface and affect the epidermal layer of the skin, broad-spectrum sunscreens are designed to block rays in the UVB and UVA wavelengths [3–5]. UVB rays, while less common on Earth's surface than UVA rays, have a shorter wavelength and higher energy than UVA rays, and therefore are capable of greater damage to the skin. UVB exposure to the skin can cause mild to severe erythema, typically referred to as sunburn or suntanning, as well as photoaging via collagen degeneration and abnormal deposition of elastic fibers of the skin [6]. In extreme cases, prolonged and unprotected exposure to UVA and UVB can result in damage to a cell's DNA which can result in uncontrolled cell growth and skin cancer. While exposure to UVB radiation has been identified as the major contributor to the more harmful effects of solar radiation, studies revealed detrimental effects of long-term exposure to UVA radiation as well.

While natural mechanisms for short-term UV protection exist (i e., melanin), long-term UV exposure to the skin must be protected using broad-spectrum sunscreens. Since UV exposure has been attributed to skin aging, more people have committed to frequent use of sunscreens in their skincare routines. As a result, sunscreens are in high demand, and synthesis of effective and safe, broad-spectrum, organic or inorganic UV-blocking compounds is an ever-growing industrial field of chemistry. The selection of UV filters is based on the chemical and physical properties of the compounds present in the filter that contribute to absorption, reflection, or diffusion of UV radiation.

The extent and range in which an organic UV filter absorbs UV radiation is dependent upon the ingredient's chemical structure. The mechanism of an organic filter involves the absorption of energy via chromophores, which are unsaturated atoms or functional groups responsible for absorbing and reflecting light at a distinct angle. The chromophores present in the organic filters undergo a delocalization of the π-electrons in highly conjugated systems, in which the molecule goes from the ground state to an excited state (HOMO to LUMO) [7–9]. The energy of the UV light is conveniently converted into infrared energy, or heat, through absorption by the conjugated system of electrons.

Cinnamaldehyde derivatives show great promise as organic UV filters due to their absorbance abilities within the UV range. Common characteristics of organic UV filters include a high degree of conjugation and large molar absorptivity (ε). In this project, five cinnamaldehyde-derived organic compounds were synthesized with cyclic and noncyclic ketones via the aldol condensation reaction to yield highly conjugated α, β-unsaturated ketones as shown in Figure 1.

After synthesizing the UV-absorbing compounds, they were analyzed by nuclear magnetic resonance (NMR) and attenuated total reflection Fourier-transform infrared (FTIR) spectroscopies to verify their identities as dialdol products. Samples of the compounds were then analyzed using ultraviolet-visible (UV-vis) spectroscopy to determine their individual ranges and intensities of UV absorption.

A new wave of cosmetics focuses on utilizing ingredients that protect the approximately 1000 species of beneficial bacteria of the cutaneous microbiota that correlate with healthy skin and even an enhanced immune response [8–10]. To assess the safety of the potential UV filters as cosmetic ingredients, it was also important to investigate the effect of each compound on bacteria that support human health [11, 12]. In order to analyze the potential effects, the synthesized compounds were mixed with cultures of *Pseudomonas aeruginosa,* one of the bacterial species that coexists on the dermis. *P. aeruginosa* is a Gram-negative bacillus that colonizes skin as an opportunistic pathogen but produces 4-hydroxy-2-heptylquinolone-*N*-oxide, which prevents the overgrowth of *Staphylococcus aureus*, another opportunistic Gram-positive coccus associated with antibiotic resistance infections of MRSA. Organic UV-blocking compounds were dissolved in DMSO, mixed with *P. aeruginosa* culture, and applied to agar plates in a time-course bacteria growth spot assay to determine the effects of the compounds on typical skin bacteria.

2. Methods and Materials

2.1. Instruments, Materials, and Reagents. All NMR spectra were obtained using a Bruker Fourier 300 MHz NMR with $CDCl_3$ solvent. Each experimental chemical shift was compared to literature values from a spectra database for organic compounds, published Gottlieb et al. [13]. Predicted NMR spectra for each synthesized compound were produced for comparison to theoretical spectra using the ChemDraw professional software from PerkinElmer. The ATR-FTIR spectra were collected using a Bruker Tensor 27 FTIR spectrometer. Prominent ATR-FTIR peaks were characterized by comparing the wave number to reference tables published on the Millipore Sigma-Aldrich website and reference spectra on the NIST database [13, 14]. UV-vis spectra were collected using a Hewlett-Packard 8463 UV-vis spectrometer. Each sample was dissolved in ethanol to 0.025 mM prior to measuring UV absorption. The molar absorptivity (ε) of each compound was determined using the absorption values in conjunction with the BeerLambert Law equation, in which the molar absorptivity (ε) equals the absorbance (A) divided by the concentration (c) of the analyte times the pathlength (l) of the light ($\varepsilon = \mathrm{A/c} * \mathrm{l}$).

The cinnamaldehyde derivatives, ketone reagents, acetone, ethanol, ethyl actetate, DMSO, and $CDCl_3$ used in the synthesis reactions were purchased from Thermo Fisher Scientific. Thin-layer chromatography (TLC) was performed using silica glass gel plates. Each plate was stained in phosphomolybdic acid (PMA) solution and viewed with UV active light.

P. aeruginosa used for the biological assay were cultured in Terrific broth (TB; KD Medical, #BLF-7170) and grown on tryptic soy agar (Difco, #236940). The solvent used for the organic filters in the biological assay was DMSO (Consolidated Chemicals and Solvents, #67-68-5). Kanamycin A derived from *Streptomyces kanamycetious* antibiotic (Sigma-Aldrich, #K-4000) was used as a control inhibitor of bacterial growth for the spot assays. To detect surface presence of organic compounds on agar plates in the spot assay, imaging was completed using a Nikon Eclipse Ti-2 confocal microscope supported by the NIS Elements AR 5.00.00 64 bit software. Bacterial growth was measured on a UVP BioSpectrum 810 Imaging System with 365 nm epi illumination, and area densities were measured with Life Science Vision Works LS Image Acquisition and Analysis software version 8.1.2.

2.2. General Synthetic Methods. A cinnamaldehyde derivative was combined with acetone at room temperature. In a separate Erlenmeyer flask, sodium hydroxide pellets, fully dissolved in deionized water and ethanol, were cooled to 20°C. Two milliliters of cinnamaldehyde derivative-acetone solution were added and stirred at room temperature for 15 minutes, before adding the remaining cinnamaldehyde

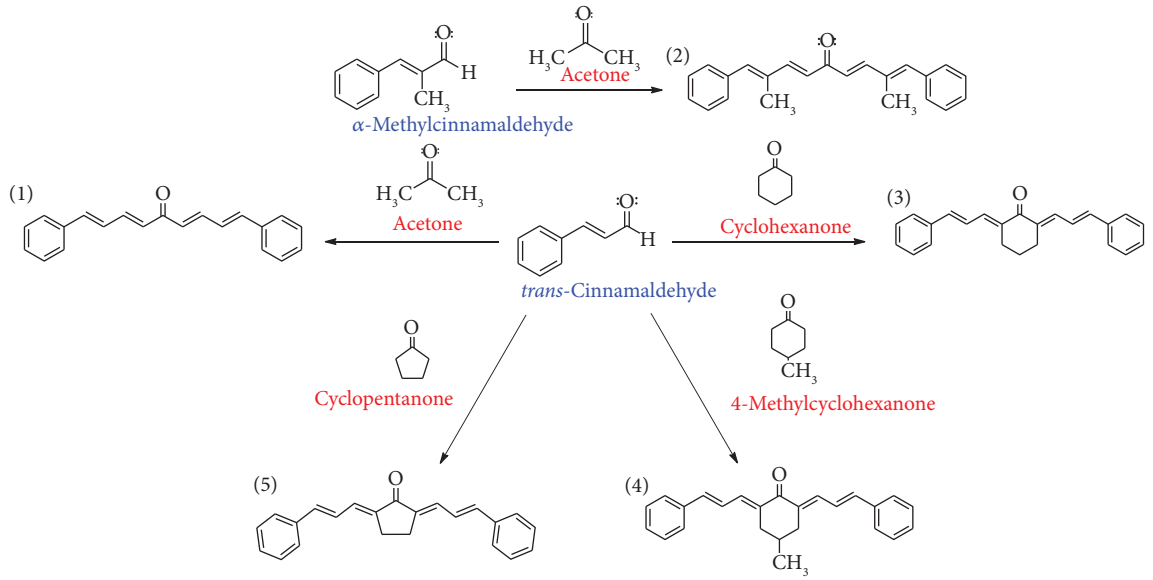

Figure 1: Five cinnamaldehyde-derived organic compounds (1–5) were synthesized with cyclic and noncyclic ketones via the aldol condensation reaction.

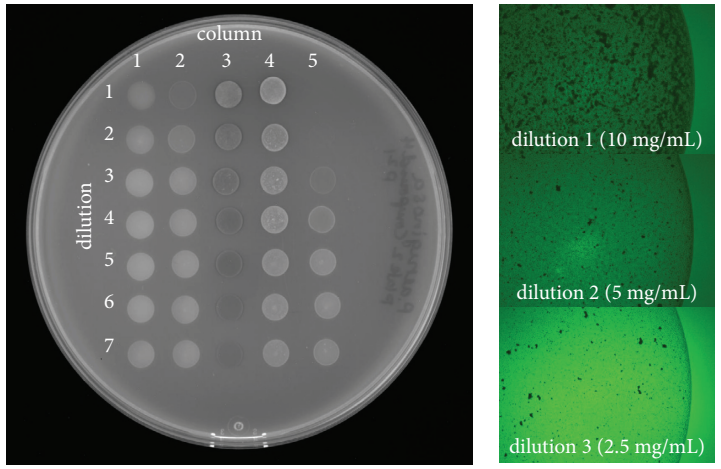

Figure 2: A representative bacterial growth spot assay on a tryptic soy agar culture plate imaged with epi illumination at 365 nm. 5 μL of mixtures were spotted down columns 1, 2, 4, and 5 with the highest concentration at dilution 1 and the lowest concentration at dilution 7. (a) Column 1 was *P. aeruginosa* with TB (TB+); column 2 was *P. aeruginosa* with DMSO (DMSO+); column 3 was dissolved UV compound in DMSO without bacteria (UV compound + DMSO−); column 4 was *P. aeruginosa* with UV compound in DMSO (UV compound + DMSO+); and column 5 was *P. aeruginosa* with kanamycin antibiotic (kanamycin+). (b) Representative microscopic imaging of UV filter residue physically occupying tryptic soy agar surface.

derivative-acetone solution and stirring for another 30 minutes. The yellow precipitate was collected by suction filtration. The precipitate was transferred to a beaker, washed with deionized water, and filtered again by suction filtration. The crude product was recrystallized using ethanol, filtered by suction filtration, and rinsed with cold ethanol. The recrystallized product was then chromatographed on silica gel and eluted, and its melting point was measured. Specific synthesis procedures for all five compounds are given with the supplementary material. Spectroscopic data, 13C-NMR, 1H-NMR, ATR-FTIR, and UV-vis for all five compounds are in the supplementary materials in Figure 1(a) to 20(a). The spectroscopic information for 13C-NMR, 1H-NMR, ATR-FTIR, and UV-vis for all five compounds is summarized in Tables 1(a) to 10(a) in the supplementary materials.

2.3. Bacterial Growth Spot Assay. For each of the five potential UV filter compounds, data were collected in time-course spot assays to assess the growth of *P. aeruginosa* by comparing five conditions at seven 2-fold dilutions for six hours (see Supplemental Materials, Table 12(a)). The five

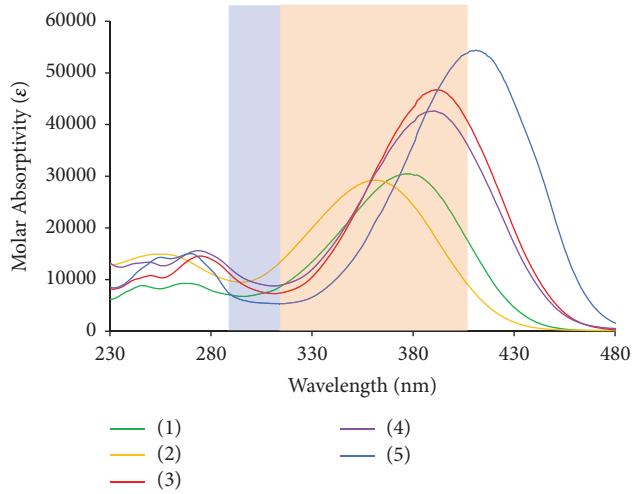

Figure 3: Combined UV-vis spectra for all of the synthesized organic UV filters in 95% ethanol solution, where the blue region represents the UVB range (290–320 nm) and the orange region represents the UVA range (320–400 nm).

Table 1: Calculated molar absorptivity (ε) in 95% ethanol of $p \longrightarrow \pi^*$ transition peak for each synthesized sunscreen product.

Compound	Molar absorptivity ($L \times mol^{-1} \times cm^{-1}$)
1	30,458
2	29,227
3	46,730
4	42,630
5	54,426

Table 2: Effective absorbance ranges of five cinnamaldehyde derivatives. FWHM is full-width at half maximum absorbance. HWHM is half-width at half maximum absorbance.

Compound	λ_{max} (nm)	Absorption range (FWHM)	Δ FWHM (−)	Δ (nm) FWHM (+)	Absorption range (HWHM)	Δ HWHM (−)	Δ (nm) HWHM (+)
1	377.3	327.1 to 414.5 nm	50.2	37.2 nm	352.2 to 395.9 nm	25.1	18.6 nm
2	361.5	321.5 to 398.7 nm	40.0	37.2 nm	341.5 to 398.7 nm	20.0	18.6 nm
3	392.0	350.6 to 422.6 nm	41.4	30.6 nm	371.3 to 407.3 nm	20.7	15.3 nm
4	391.2	349.2 to 426.0 nm	42.0	34.8 nm	370.2 to 408.6 nm	21.0	17.4 nm
5	410.8	368.2 to 446.6 nm	42.6	35.8 nm	389.5 to 428.7 nm	21.3	17.9 nm

conditions compared were as follows: column (1) *P. aeruginosa* mixed with TB alone (no DMSO, no UV filter, no inhibitor; TB+); column (2) *P. aeruginosa* mixed with DMSO (solvent effect, no UV filter, no inhibitor; DMSO+); column (3) UV filter in DMSO alone (UV filter effect, no bacteria, no inhibitor; UV + DMSO−); column (4) *P. aeruginosa* mixed with UV filter dissolved in DMSO (UV filter + DMSO effect, no inhibitor; UV + DMSO+); and column (5) *P. aeruginosa* mixed with kanamycin A (known inhibitor effect, no UV filter, no DMSO; kanamycin+). The representative spot assay plate shown in Figure 2 assessed bacterial growth in the presence of compound 4 after three hours of incubation at 37°C. Detailed steps for prepared spot assay plates, measuring area densities, and data analysis for the biological assays can be found in the Supplementary Materials.

3. Results and Discussion

3.1. UV-Visible Absorption and Molar Absorptivity. UV-vis spectra of each synthesized sunscreen product were measured, as shown in Figure 3. The absorbance of each maximum peak was converted to molar absorptivity (ε) using the Beer–Lambert Law (Table 1) as well as absorbance ranges determined by full-width at half maximum peak absorbance (FWHM) and half-width at half maximum peak absorbance (Table 2). The most effective ranges of wavelengths that would absorb radiation by the cinnamaldehyde derivative compounds were determined by peak molar absorptivity (λ_{max}) as well as ranges determined by full-width at half maximum peak absorbance (FWHM) and half-width at half maximum peak absorbance (Table 2). According to the absorbance ranges, all five compounds

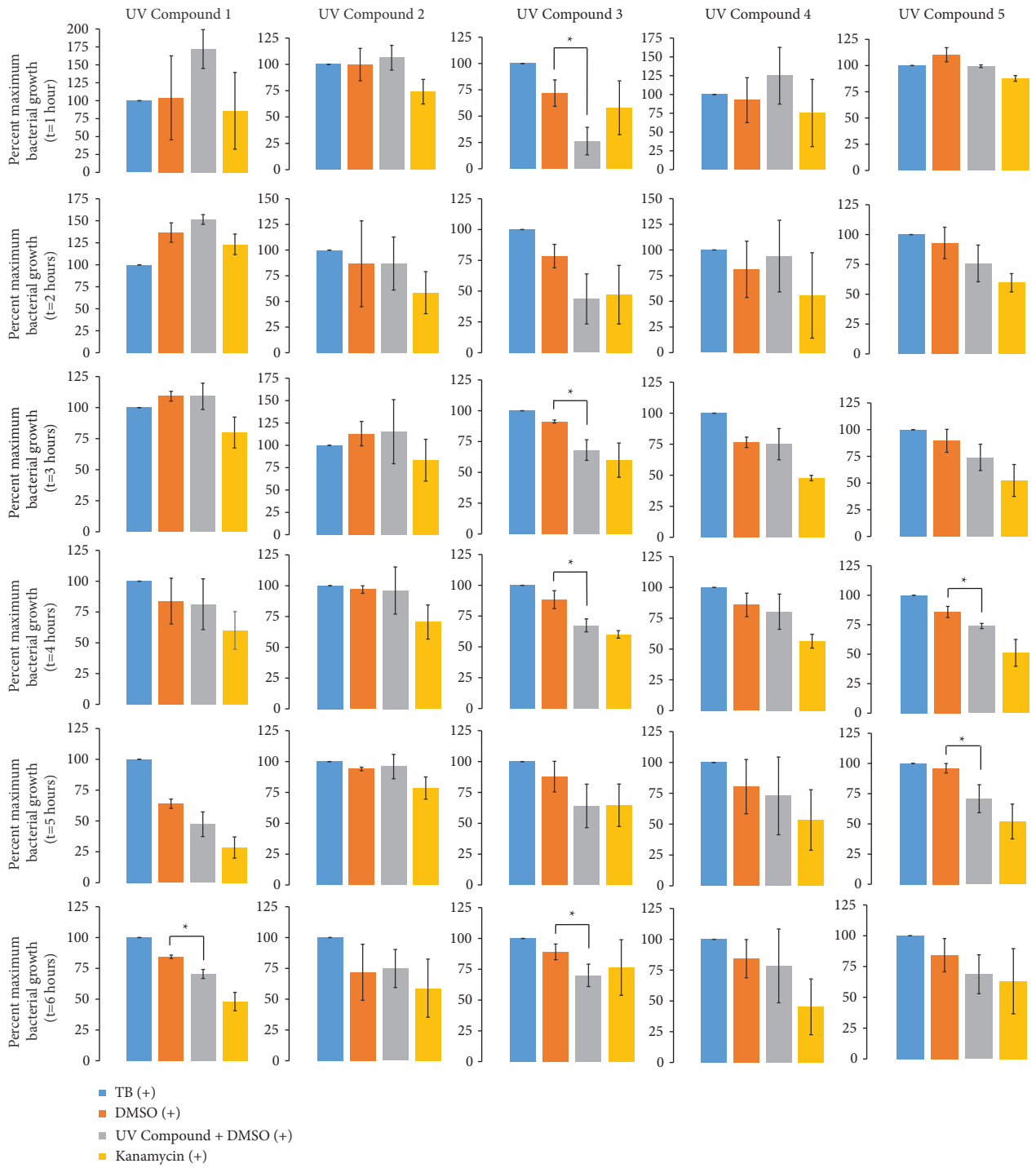

Figure 4: Time-course analysis of bacterial growth. *P. aeruginosa* growth at 1/16 dilutions over six hours of incubation at 37°C at one-hour intervals expressed as percent maximum where growth at 100% is represented by TB+ ($n = 4$ for UV compound 1 and $n = 3$ for UV compounds 2–5). Experimental conditions compared TB combined with *P. aeruginosa* culture (light blue, TB+), DMSO combined with *P. aeruginosa* (red, DMSO+), compound dissolved in DMSO combined with *P. aeruginosa* (gray, UV compound + DMSO+), kanamycin combined with *P. aeruginosa* (yellow, kanamycin+), and compound combined with DMSO without the presence of *P. aeruginosa* (dark blue, UV compound + DMSO−). Significant differences are indicated between DMSO+ and UV compound + DMSO+ with an asterisk ($p < 0.05$).

cover the UVA range, compound 2 covers small amount of UVB range, and none of the compound covers the UVC range. Each organic UV filter was dissolved in 95% ethanol and added to a 1 cm wide quartz cuvette. Of the five compounds, it was determined that compound 5 had the largest molar absorptivity value of 54,426 L mol^{-1} cm^{-1}, which measures how well a chemical compound is capable of absorbing a given wavelength of light [15, 16]. Given that

compound 5 had the largest molar absorptivity value, this compound would be the most efficient organic UV filter for absorbing harmful UV rays. Though compound 5 is a stronger sunscreen agent, it fails to cover the UVB range and only covers within the UVA range. Compound 3 and compound 4 cover the UVA range and both compounds show potential as UVA filters due to their relatively high molar absorptivity values. Compound 1 and compound 2 were observed to cover the entire UVA region. These two compounds may be capable of covering UVA range and have relatively large molar absorptivity values of 30,458 and 29,227 $\mathrm{L\,mol^{-1}\,cm^{-1}}$, respectively. As published in the *Journal of Dermatological Therapy*, UV filters present in sunscreens have a molar extinction coefficient of up to 20,000 $\mathrm{L\,mol^{-1}\,cm^{-1}}$ and are considered effective for use in commercial sunscreens [17].

Each organic UV filter shows potential as an active sunscreen ingredient for UVA protection; however, they provide little-to-no potential as broad-spectrum sunscreen ingredients.

For these synthesized organic filters, the UV-vis spectrum reveals the presence of $n \longrightarrow \pi^*$ and $p \longrightarrow \pi^*$ transition peaks, as shown in Figure 3. The molar extinction coefficient used to determine each compound's potential as a UV filter was based on the $p \longrightarrow \pi^*$ peaks, or the peaks with the highest molar absorptivity. The other peaks present at lower wavelengths with low extinction coefficients represent the $n \longrightarrow \pi^*$ transitions that are a result of intramolecular charge-transfer transition involving the carbonyl group [18].

3.2. Detecting Bacterial Growth Inhibition over Time. The fourth dilution in the 2-fold dilution series of spots was selected to determine changes in the exponential growth phase of the bacteria, as described in the Supplementary Materials Figure 21(a). Bacterial growth was then compared over 6 hours of incubation at one-hour intervals, as shown in Figure 4.

The nature of bacterial growth in the presence of each cinnamaldehyde derivative aldol compounds dissolved in DMSO were directly compared to DMS solvent effects alone ($n = 4$ for UV compound 1; $n = 3$ for UV compounds 2–5). Significant decreases in bacterial growth between DMSO solvent alone (DMSO+) and the presence of both DMSO and UV compound were determined by a Student's t-test Figure 4; $^* p < 0.05$. These conditions were flanked by ideal *P. aeruginosa* growth in Terrific broth (TB+) as a positive control (establishing the 100% maximum bacterial growth measure in Figure 4) and in the presence of the antibiotic kanamycin (kanamycin+) as a control for inhibited growth. While kanamycin is a known inhibitor of *P. aeruginosa*, suboptimal concentrations of this antibiotic can result in antibiotic resistant forms while inducing biofilm formation of the bacteria and enhanced toxin production [19]. Based on our collected data, concentrations of kanamycin less than 12.5 mg/mL under conditions presented in the spot assays allowed for delayed growth of *P. aeruginosa*. Most measures of these two controls resulted in significant differences between bacterial growth in TB versus in the presence of kanamycin, but were not indicated in Figure 4 in order to focus on relevant experimental differences between bacteria grown in DMSO solvent alone versus in the presence of UV compound dissolved in DMSO.

While compounds 2 and 4 showed no significant decrease in bacterial growth at any time point up to 6 hours, a significant decrease in growth emerged in the presence of UV compound 1 at 6 hours. Since bacterial growth in the presence of UV compound 1 differed from DMSO only after 6 hours, it is unclear whether the difference would have continued if measures were continued into the seventh hour and longer times of incubation. Growth in the presence of UV compound 3 was significantly diminished at 1 hour, 3 hours, 4 hours, and 6 hours. These results suggest antimicrobial properties of UV compound 3 on bacterial growth of *P. aeruginosa*, yet mean bacterial growth in the presence of UV compound 3 after 6 hours still measured at 70.0% ± 9.1% relative to ideal growth in TB. Therefore, it is unclear if the results represent true inhibition or simply delayed bacterial growth. Growth in the presence of UV compound 5 was significantly diminished when measured after 4 hours and 5 hours of incubation. Since two consecutive measures indicated significant differences, assessment of bacterial growth inhibition was further investigated for UV compound 5 along with UV compound 3.

Closer analysis of potential growth inhibition comparing TB+, DMSO+, UV compound+, and kanamycin+ for compounds 3 and 5 suggested growth inhibition was either competitive or mixed when using double reciprocal plots (see Supplementary Materials, Figure 22(a)). Considering microscopic images indicated the UV filters remained at the surface of the agar plates (Figure 2(b)), it is likely any delay in bacterial growth may have been due to simple niche competition; that is, the bacteria lost surface area on which to initiate growth where the UV filter occupied space.

4. Conclusion

Five organic UV filters were synthesized and characterized through NMR, ATR-FTIR, and UV-vis analyses. Based on the UV-vis spectra, each compound was determined to have a high molar absorptivity capable of absorption within the UVA range, revealing each filter's potential as an active sunscreen ingredient. Current UV filters are reported to have molar absorptivity values of up to 20,000 $\mathrm{L\,mol^{-1}\,cm^{-1}}$, while the synthesized organic filters from this project ranged from 29,000 to 54,000 $\mathrm{L\,mol^{-1}\,cm^{-1}}$, indicating the relative UV absorption effectiveness of the compounds. According to the time-course and concentration gradient bacterial growth assay, compounds 1, 2, and 4 caused no growth inhibition of *P. aeruginosa*, but compounds 3 and 5 indicated modest bacterial growth delay that resembled typical growth inhibition of growth with suboptimal doses of kanamycin. These results support that the synthesized organic UV filters are strong candidate sunscreen ingredients.

The next stage of this project may involve investigation of the safety and effectiveness of the UV blockers by further researching the degradation and photostability of each organic UV blocker to determine the shelf life of the

compounds. Environmental persistence of sunscreen ingredients has gained recent attention with oxybenzone and octinoxate recently rendered illegal as of January 1, 2021, in the Hawaiian islands due to underwater habitat destruction of coral reefs [20]. Although organic compounds may interact with high affinity to skin cells, it is unclear whether these would eventually aggregate in freshwater or marine environments with natural shedding of dead skin cells. Therefore, persistence of the cinnamaldehyde derivative aldol UV filters synthesized for this experiment should be assessed in varied environments before distribution to avoid additional damage to precious habitats.

In this experiment, modest inhibitory effects were found in the presence of two of the cinnamaldehyde derivative aldol UV filters on the bacterial growth of *P. aeruginosa*. Assessing changes in bacterial growth of *Staphylococcus epidermidis* and *Staphylococcus aureus* in the presence of the cinnamaldehyde derivative aldol compounds would further indicate any disturbance to the balance of epidermal microbiota.

Data Availability

The NMR data used to support the findings of this study are included within the supplementary information files.

Conflicts of Interest

The authors declare that they have no conflicts of interest.

Acknowledgments

This work was supported by the Austin Peay State University Chemistry Department's operating budget.

Supplementary Materials

This section includes the specific synthesis procedures for all five compounds. Figures 1(a) to 20(a): 13C-NMR, 1H-NMR, ATR-FTIR, and UV-vis spectroscopic data, for all five compounds. Tables 1(a) to 10(a): the spectroscopic information. (*Supplementary Materials*)

References

[1] M. N. Mead, "Benefits of sunlight: a bright spot for human health," *Environmental Health Perspective*, s, vol. 116, 2008.

[2] R. Stokes, "Project Sunscreen Protection," in *Dermatopharmacology of Topical Preparations*, B. Gabard, C. Surber, and P. Elsner, Eds., Springer, Berlin, Heidelberg, pp. 365–382, 2000.

[3] S. Forestier, "Rational for sunscreen development," *Am. Acad. Dermatol.*vol. 58, no. 5, pp. 133–138, 2008.

[4] B. D. Wilson, S. Moon, and F. Armstrong, "Comprehensive review of ultraviolet radiation and the current status on sunscreens," *Clin. Aesthet. Dermatol.*vol. 5, no. 9, pp. 18–23, 2012.

[5] F. de la Coba, J. Aguilera, N. Korbee et al., "UVA and UVB photoprotective capabilities of topical formulations containing mycosporine-like amino acids (Maas) through different biological effective protection factors (BEPFs)," *Marine Drugs*, vol. 17, no. 1, 2019.

[6] Y. Tu and T. Quan, "Oxidative stress and human skin connective tissue aging," *Cosmetics*, vol. 3, no. 3, pp. 1–12, 2016.

[7] D. R. Kimbrough, "The photochemistry of sunscreens," *Journal of Chemical Education*, vol. 74, no. 1, pp. 51–53, 1997.

[8] M. S. Cosmetics, "The next microbiome Frontier," *C&EN*, vol. 95, no. 19, pp. 30–34, 2017.

[9] R. L. Gallo and S. Epidermidis, "influence on host immunity: more than skin deep," *Cell Host & Microbe*, vol. 17, no. 2, pp. 143-144, 2015.

[10] L. R. Hoffman, E. Deziel, D. A. D'Argenio et al., "Selection for *Staphylococcus aureus* small-colony variants due to growth in the presence of *Pseudomonas aeruginosa*," *Proceedings of the National Academy of Sciences*, vol. 103, no. 52, pp. 19890–19895, 2006.

[11] S. G. Kazarian and K. L. A. Chan, "Application of ATR-FTIR spectroscopic imagining to biomedical samples," *Biochimica et Biophysica Acta (BBA) - Biomembranes*, vol. 1758, no. 7, pp. 853–867, 2006.

[12] R. D. Rundel, "Action spectra and estimation of biologically effective UV radiation," *Physiologia Plantarum*, vol. 58, no. 3, pp. 360–366, 1983.

[13] H. E. Gottlieb, V. Kotlyar, and A. Nudelman, "NMR chemical shifts of common laboratory solvents as trace impurities," *Journal of Organic Chemistry*, vol. 62, no. 21, pp. 7512–7515, 1997.

[14] Spectrum Table and Chart, https://www.sigmaaldrich.com/technical-documents/articles/biology/ir-spectrum-table, 2020.

[15] S. McMurry and J. McMurry, *Organic Chemistry*John McMurry, Belmont, CA, USA, 2016.

[16] W. Reusch, "Visible and Ultraviolet Spectroscopy," 2020.

[17] R. Wolf, B. Tuzun, and Y. Tuzun, "Sunscreens," *Dermatologic Therapy*, vol. 14, no. 3, pp. 208–214, 2001.

[18] B. A. M. Corrêa, A. S. Gonçalves, A. M. T. De Souza et al., "Molecular modeling studies of the structural, electronic, and UV absorption properties of benzophenone derivatives," *The Journal of Physical Chemistry A*, vol. 116, no. 45, Article ID 10927, 2012.

[19] C. Jones, L. Allsopp, J. Horlick, H. Kulasekara, and A. Filloux, "Subinhibitory concentration of kanamycin induces the *Pseudomonas aeruginosa* type VI secretion system," *PLoS One*, vol. 8, no. 11, Article ID e81132, 2013.

[20] C. Jones, *Policy SB2571, the Senate, Twenty-Ninth Legislature*, Hawaii, USA, 2018.